Published in final edited form as:
Anal Chim Acta. 2013 March 20; 768: 129–135. doi:10.1016/j.aca.2013.01.029.

A Disposable Blood Cyanide Sensor

Yong Tian[1,2], **Purnendu K. Dasgupta**[1,*], **Sari B. Mahon**[3], **Jian Ma**[1], **Matthew Brenner**[3], **Jian-Hua Wang**[2], and **Gerry R. Boss**[4]

[1]Department of Chemistry and Biochemistry, University of Texas at Arlington, 700 Planetarium Place, Arlington, TX 76019-0065, USA

[2]Research Center for Analytical Sciences, Northeastern University, Box 332, Shenyang 110819, China

[3]Beckman Laser Institute, University of California, Irvine, Irvine, CA, 92612-1475, USA

[4]Department of Medicine, University of California, San Diego, La Jolla, CA 92093-0652, USA

Abstract

Deaths due to smoke inhalation in fires are often due to poisoning by HCN. Rapid administration of antidotes can result in complete resuscitation of the patient but judicious dosing requires the knowledge of the level of cyanide exposure. Rapid sensitive means for blood cyanide quantitation are needed. Hydroxocyanocobinamide (OH(CN)Cbi) reacts with cyanide rapidly; this is accompanied by a large spectral change. The disposable device consists of a pair of nested petri dish bottoms and a single top that fits the outer bottom dish. The top cover has a diametrically strung porous polypropylene membrane tube filled with aqueous OH(CN)Cbi. One end of the tube terminates in an amber (583 nm) light emitting diode; the other end in a photodiode via an acrylic optical fiber. An aliquot of the blood sample is put in the inner dish, the assembly covered and acid is added through a port in the cover. Evolved HCN diffuses into the OH(CN)Cbi solution and the absorbance in the long path porous membrane tube cell is measured within 160s. The LOD was 0.047, 1.0, 0.15, 5.0 and 2.2 μM, respectively, for water (1 mL), bovine blood (100 μL, 1 mL), and rabbit blood (20μL, 50 μL). RSDs were < 10% in all cases and the linear range extended from 0.5 to 200 μM. The method was validated against a microdiffusion approach and applied to the measurement of cyanide in rabbit and human blood. The disposable device permits field measurement of blood cyanide in < 4 min.

Keywords

Porous membrane; HCN; Cobinamide; Liquid Core Waveguide

1. Introduction

Cyanide exists widely in the environment [1–3]. More than 2000 microbes and plants (e.g., bacteria, fungi, algae, cassava, lima beans, sorghum, linseed, fruit kernels, sweet potatoes, and bamboo shoots) produce cyanide or cyanogenic compounds as defense against pests or through metabolism of nitrogenous foods [4, 5]. Except for cassava root [6] and possibly

*Corresponding author: Dasgupta@uta.edu, phone 817 272 3806.

Pseudomonas aeruginosa, most plant/microbial production of HCN does not pose a health hazard. Several billion tons of cyanide are industrially produced and used each year in pesticides, electroplating, metallurgy, mining, and production of organic chemicals and polymers [5, 7]. Acrylonitrile is the most common carpet fiber; large amounts of HCN are produced in fires. The majority of deaths from fire occur due to smoke inhalation, and many are attributable to cyanide poisoning [8]. Cyanide is also a potential weapon of terrorism and has already been so used [9, 10]. Cyanide rapidly arrests cellular respiration; it is imperative that cyanide-poisoned subjects are diagnosed and treated quickly. Both for diagnosis and appropriate antidote dosing, blood cyanide levels must be readily measured. A simple, field-deployable blood cyanide measurement device that can rapidly measure cyanide in blood with reasonable accuracy is much needed.

Cyanide measurement methods have been recently reviewed [11–14]; the accuracy of blood cyanide measurements has been especially questioned [14]. Presently, gas chromatography (GC) with mass spectrometric, nitrogen selective or electron capture detection is most commonly used [15–22]. Obviously blood cannot be directly injected; sample manipulation is slow; the GC methods are not presently field-usable. Other methods have also been used to detect cyanide in blood. Lindsay et al. used a Nafion-coated gold electrode for amperometric determination of blood cyanide; this approach is convenient but the limit of detection (LOD) was not sufficient for the intended clinical field use [23]. Lv et al. [24] used a mini-distiller to liberate and collect HCN followed by flow-based detection of the cyanide by the Cu(II)-CN^--luminol chemiluminescence reaction. Blackledge et al. [25] used the color reaction between cyanide and aquohydroxocobinamide (H_2O(OH)Cbi) to measure cyanide in rabbit blood using microdiffusion over a long period. None of these methods are field-usable. We previously attempted to use the H_2O(OH)Cbi chemistry [26] for blood cyanide measurement [27] by pipetting the blood sample (0.2 – 1 mL) into a screw-top microcentrifuge tube, adding a defoamer (ethanol), sealing the tube with a special top that has a light source and a H_2O(OH)Cbi impregnated filter, adding H_3PO_4 via a syringe to liberate HCN and then bubbling air through the mixture to purge the HCN from solution. The liberated HCN proceeded through a Cbi reagent impregnated filter whose absorbance was continuously measured with an LED and a photodiode. This provided the requisite sensitivity and could be used in non-emergency situations. For emergency field use, experience indicates that a method with fewer steps is needed. The need to bubble air to displace HCN clearly sets a lower limit on the sample volume and one must be careful about bubbling rate, else foam reaches the sensor top (foaming of blood could not be prevented by conventional silicone-based anti-foam agents). Appropriate storage and formulation of the filter is critical –the reaction with HCN is affected both by pH and the filter moisture content – a dry filter reacts poorly. Ideally, a finger prick should be sufficient to provide the necessary sample (≤ 50 μL) for analysis: This method falls far short of that goal.

A greater understanding of Cbi chemistry has since emerged [28]. The transformation of CN(H_2O)Cbi to $(CN)_2Cbi^-$ actually produces a much greater color change than the transformation of OH(H_2O)Cbi to CN(H_2O)Cbi. With better understanding of the chemistry, we devise here a sensor (disposable in principle) based on CN(H_2O)Cbi that uses a liquid core waveguide (LCW)–like detection geometry. The detector geometry provides a significant path length and excellent sensitivity. The LCW is composed of a HCN permeable porous hydrophobic membrane tube that is close to the sample surface, obviating the need for gas purging and permitting very small sample volumes.

2. Experimental

2.1. Reagents and samples

All chemicals used were reagent grade or better. 18 MΩ•cm Milli-Q water (www.Millipore.com) was used throughout. Aquohydroxocobinamide was synthesized as described in [25]. A stock solution of $H_2O(OH)Cbi$ was prepared by dissolving the solid in water (1 mM). This can bind two cyanide ions but the spectral change is greater in going from the $OH(CN)Cbi^-$ to $(CN)_2Cbi^-$ rather than the transition from $H_2O(OH)Cbi$ to $OH(CN)Cbi^-$ [28]. We therefore used $OH(CN)Cbi^-$ as the color reagent; 1 mmol KCN was added per mmol of $H_2O(OH)Cbi$ and stored overnight or longer to make $OH(CN)Cbi^-$. A working solution of 20 μM $OH(CN)Cbi^-$ was prepared by diluting the stock solution with 0.01 M borate buffer (10 mmol $Na_2B_4O_7{\cdot}10\ H_2O$ in 1 L H_2O, adjusting pH to 10.0 with 2 M NaOH). Cyanide stock solutions were prepared by dissolving KCN in 1 M NaOH and stored refrigerated at 4 • • [26–29]. Defibrinated bovine and rabbit blood (R100-0100 and R109-0100, respectively, www.rockland-inc.com) was used as “blank” blood samples, with appropriate amounts used for experimental optimization and performance evaluation.

Blood samples from experimental animals were obtained from ongoing studies of cyanide poisoning at the University of California, Irvine (UCI). These studies follow the NIH Guidelines for the Care and Use of Laboratory Animals and are approved by the UCI Institutional Animal Care and Use Committee. The samples were divided, with half analyzed at the University of California, San Diego (UCSD) according to a microdiffusion procedure [25] adapted after the Conway microdiffusion approach [30–33] and the other half analyzed according to the present method. Blood from 12 healthy human volunteers was obtained according to a protocol approved by the Institutional Review Board at the University of Texas at Arlington and analyzed by the present method.

2.2. Device construction

Referring to Figure 1 and Figure S1 in the SI, an L-shaped liquid passage pathway was machined into a 583 nm light emitting diode (LED, 5 mm φ, 516-1336-ND, www.digikey.com) and the terminal diameter was machined to ~2 mm as illustrated. This LED functioned as the light source and was powered by a 5 V supply with an adjustable resistor to limit the current to 20 mA. Two holes are made on opposite sides of a 50 mm dia. Petri-dish cover; the LED is fixed on one hole. The LED end is push-fit into a ~50 mm long porous polypropylene membrane tube (PPMT, Accurel PP, 1.8 mm i.d., 0.45 mm wall, www.membrana.de). A 2 mm dia. acrylic optical fiber OF was pushed though the opposite hole and push fit into the free PPMT end. With the PPMT stretched taut, the PPMT/OF was also fixed on the cover (hot-melt adhesive). The OF end contained the same L-shaped aperture as the LED; these apertures in the LED and OF allow simple liquid in/out connections without additional tee’s and greatly simplify design. Such apertures would be easily molded in mass-manufactured devices. While some light is lost (a 0.64 mm dia. aperture represents 10% of the area of a 2 mm φ area), present-day LED-detector combinations do not even need the LEDs to be powered at the maximum permissible current for sufficient light intensity at the detector. The far end of OF was coupled to light to voltage converter (TSL257, www.taosinc.com). Putting the sample dish on a compressible foam block positions the top dish firmly against the interior cover of the box. The umbilical cord from the disposable sensor to the processing electronics has four lines, power supply lines to both LED and detector, common ground and detector signal, acquired by a 14-bit USB-based data acquisition (DAQ) board (USB-1408FS, www.mccdaq.com) filtered by a 1 s RC filter.

The sample container is a 30 mm i.d.x10 mm tall Petri-dish bottom affixed concentrically in a 54 mm i.d. x 15 mm tall Petri-dish bottom. The top cover with the opto-membrane assembly completes the arrangement; it is placed in a dark enclosure (may be shared with the electronics, Figure S1). The enclosure top provides a sealed Luer port for introducing acid directly into the sample container. A laptop computer powered the DAQ and acquired the data.

2.3. Operation sequence

The dark signal (I_d) was initially acquired with the LED off. Blood (20–1000 μL) is pipetted into the dish (Figure S3), the cover was closed, and the PPMT was filled with $OH(CN)Cbi^-$ solution. The LED was turned on (t = 0); the average reading during 50–60 s taken (I_0). At 60 s, ~2 mL of 30% H_3PO_4 was introduced through the Luer top to release HCN. Data acquisition is continued through at least next 100 s. The released HCN is captured by the $OH(CN)Cbi^-$ in the PPMT and increases optical absorption at 583 nm. The detector signal is recorded as I_t.

2.4. Caution

The amount of cyanide used in these studies does not pose a major hazard. However, diluted bleach (which oxidizes cyanide immediately) should always be kept in reach in case of accidental spill of stock cyanide solutions.

2.5. Data analysis

A water-filled hydrophobic porous tube is a good light conductor [34], akin to an LCW. When an aqueous solution is filled in such a tube, liquid-pore equilibration and stable light transmission requires a few seconds. For this reason 50 s is allowed to elapse before reading I_0. The temporal absorbance A_t was calculated as $log\ ((I_0-I_d)/(I_t-I_d))$. Except as stated, $A_{160\ s}$ was used for quantitation. The utilization of the entire temporal color development curve does improve reproducibility and the stated LOD but the single point quantitation described provided more than adequate LODs for the purpose.

3. Results and discussion

3.1. Gas diffusion, pervaporation and membraneless transfer of volatile analytes

The transfer of a volatile analyte from the sample matrix is particularly attractive when the matrix is complex (generally true for all biosamples) and incompatible with direct introduction into the analytical system. Conway's initial work involved a configuration, physically very similar to that in the present work, resembling a petri dish with a central well containing an acceptor chemical (solution) which receives and quantitatively absorbs the vapor coming off a donor (sample) solution which may have been altered in some way (e.g., increase/decrease pH) to facilitate release of the analyte in the vapor phase. The system works in a closed static environment as the top is sealed during the long collection period (hours) to ensure complete analyte capture. No membranes are obviously involved in this process.

In the flow domain, Skeggs pioneered segmented flow analysis (later commercialized as the Technicon Autoanalyzer); he also did not use membranes in measuring plasma or serum CO_2 [35, 36]. He transferred CO_2 in the acidified sample to the CO_2-free air used for segmenting the samples and subsequently reabsorbed the liberated CO_2 in the air to an indicator-bearing bicarbonate buffer. Others later chose to use membranes, however, to transfer CO_2 in similar samples when using commercial segmented flow analyzers [37]. Transfer of CO_2 in similar plasma samples was similarly accomplished early on in flow injection analysis using silicone rubber membranes [38]. Hundreds of papers since appeared

on gas diffusion flow injection analysis but it is not without its shortcomings. Strong adsorption of an analyte or a matrix component by the membrane can occur. The pores in porous membranes can be fouled. These lead to poor throughput and/or inaccurate results from changes in membrane transfer efficiency. The pervaporation technique, where a membrane is used but it is not in contact with the donor solution that can potentially foul the membrane was introduced for this reason [39]. In such a system, one pump channel is used to pump in the donor stream and another to continuously aspirate it so that a gas phase gap is maintained between the flowing donor stream and the membrane (across which the analyte is transported to the receptor. If a scheme can be devised that will permit continuous flow of both donor and acceptor streams without contact but in close vapor phase communication (in principle, much the same as a flow-through Conway cell) then the need for the membrane in the pervaporation arrangement will be obviated. Both Choengchan et al. [40] and Mornane et al. [41] independently accomplished this; the former group has since carried out other work on such “membraneless” vaporization or gas diffusion [42–45].

The static Conway cell has one advantage over flow methods: quantitative analyte transfer can be achieved. This is of significant importance if the available sample amount is low and/or trace amounts need to be measured. In field use, the fact that pumps etc. are not needed is a major advantage. The Conway cell is not a measurement device; combining a liquid core waveguide gas sensor containing a small amount of chromogenic absorbent in this sealed environment provides a novel and powerful combination of a static pervaporation sensor. Putting the sensor in close proximity of the sample donor surface provides good response kinetics. Rather than considering sample throughput on one automated analyzer, it may be a better alternative to devise sufficiently inexpensive (potentially disposable) sensors; multiple units can be deployed in parallel in the field, especially in emergencies.

3.2. Parametric influence

The optimum pH of the $OH(CN)Cbi^{-}$ absorber, and the nature/amount of the added acid were explored. The behavior of 20 μM $OH(CN)Cbi^{-}$ absorber at pH 8–13 is shown in Figure 2; quantitation was based on $A_{160\,s}$. The highest $A_{160\,s}$ was observed with a pH 10 absorber; this was henceforth used. This behavior is understandable as proton transfer equilibria is the most rapid and cyanide will not be effectively captured much below its pK_a of 9.3 while at a pH much over 10, OH^{-} competes effectively with CN^{-} for binding to the cobalt center in Cbi. However, for t ≤100 s, a pH 13 absorber provides the highest analytical absorbance; within a short period, kinetic rather than thermodynamic effects may be more important. Note also that the data in Figure 2 indicate the need for some initial stabilization time.

Cyanide in blood is tightly bound to methemoglobin (MetHb) and needs to be rapidly released. Normal dissociation rate of MetHbCN is slow; Klapper and Uchida [46] found a second order association rate constant of 180 $M^{-1}\,s^{-1}$; and association constants of 3.5 and $0.45 \times 10^{6}\ M^{-1}$ for two different binding sites. Even if we take the weaker binding site, a dissociation rate constant of $4 \times 10^{-4}\ s^{-1}$ or a dissociation half-life of 29 min is calculated. The data of Blumenthal and Kassner [47] suggest that the association constant may in fact be even higher. If so, the dissociation will be slower still. Cyanide has been determined as the fluorescent cyanobenz[f]isoindole after reacting with naphthalenedialdehyde and taurine [48,49]; after 30 min of reaction the recovery of cyanide is ~80%.

To rapidly liberate HCN from heme-bound cyanide in blood, the complex must be destroyed. Drastic conditions are required for this. Acidification had previously found to be effective; strong acids work but most cause gelation of blood and the increased viscosity slows the release of HCN from the bulk fluid. H_3PO_4 was found to be the most suitable [27]. In the present device, to obviate the need to add an acid during the assay, we initially hoped

to use an acid that could have been pre-coated on the Petri-dish. A suitable acid was not found: Sulfamic acid, thought to be the most promising, also caused gelation. We therefore returned to H_3PO_4; it did not cause gelation (Figure S2). The total liquid level influences the diffusion distance and hence the results. A constant liquid level leads to a uniform HCN release rate and a higher liquid level connotes a smaller diffusion distance to the sensor. Beyond a total volume of 3 mL, the temporal absorbance slope did not increase further. The concentration of H_3PO_4 was also studied. With 1 mL sample and 2 mL acid, 30% H_3PO_4 produced the highest absorbance slope. For sample volumes of ≤0.1 mL, 3 mL 30% H_3PO_4 was optimum. The optimized conditions for different sample volumes are summarized in Table S1.

3.3. Kinetics of color development

The release of cyanide and its subsequent capture by the $OH(CN)Cbi^-$ solution and the consequent development of color were investigated by using 2 μM cyanide spiked blood and aqueous standards. The development of color was followed for 30 min, as illustrated in Figure 3. Relative to the water blank, the "blank" bovine blood sample clearly shows measurable cyanide, this was also observed for healthy human blood samples. *A priori*, we expected color development to follow first order kinetics. However, the observed data did not fit a simple first order or second order or a consecutive first order process. On the other hand, the color development profile for both the water and blood samples closely fit a pattern where the color development proceeds through two (not necessarily equally contributing) parallel paths, one faster than the other. Such a process could be modeled as:

$$A_t = A_\infty \left[f\left(1 - e^{-k_{slow}t}\right) + (1-f)\left(1 - e^{-k_{fast}t}\right)\right] \quad (1)$$

Where A_t is the absorbance at any time t after the addition of acid, A_∞ is the projected final absorbance, f is the fraction that proceeds in the slower manner with a first order rate constant k_{slow} and $1-f$ is the fraction that proceeds in a faster fashion with a first order rate constant k_{fast}. For water, the best fit values were $A_\infty = 0.187$, $f = 0.625$, $k_{slow} = 1.36 \times 10^{-3}$ s^{-1} and $k_{fast} = 1.31 \times 10^{-2}$ s^{-1}. For blood, the best fit values were $A_\infty = 0.218$, $f = 0.494$, $k_{slow} = 1.14 \times 10^{-3}$ s^{-1} and $k_{fast} = 6.54 \times 10^{-3}$ s^{-1}. The data and the fits are shown in Figure 3. Our tentative interpretation is that HCN release from both samples can be approximated as coming from two reservoirs, one is the surface layer; the other is the bulk solution. Because of slow liquid phase diffusion, even for water there are two virtual compartments; however, the deep compartment contributes less in the case for water than for blood. For blood, the two reservoirs have virtually equal contributions. The kinetics of both the fast and slow processes have imbedded within them the kinetics of HCN formation and that of capture by the cobinamide filled membrane tube. The second contributes equally to all steps but the first must be much more rate limiting for HCN release from its heme-bound form. Accordingly, k_{fast} is only half as fast for blood as it is for water; the difference is much less rate limiting for k_{slow} where slow liquid phase diffusion has become the limiting process. We expect that the combination of a larger inner dish that will create a thinner liquid layer and a shallower outer dish (that will not increase the diffusion distance to the membrane by making the liquid layer shallower) may result in even faster color development.

3.4. System performance

Detailed performance data are summarized in Table S2 and Figures S3–S12. The determination of cyanide in water, bovine blood, and rabbit blood are discussed separately below. To put the cyanide concentrations tested here in the context of those involved in human cyanide exposures, the International Cyanide Management Code for the Gold Mining Industry [50] states the lethal human dose as 1–3 mg/kg as HCN. Cyanide exposure leads to

distribution throughout the body, including the tissues. For a 70 kg adult with total liquids (~70% of body mass) amounting to ~49 L, the estimated blood concentration will be 53–159 μM. Literature reports of cyanide levels in the blood of smoke inhalation victims are consistent with this. For 109 victims of smoke inhalation; 66 survivors and 43 fatal cases had respective mean blood cyanide levels of 21.6±36.4 and 116±89 μM, compared to 5.0±5.5 μM for unexposed control subjects [51].

Water—The calibration results for 1 mL of 0–10 μM CN^- are shown in Figure S3. The linear range (r^2> 0.99) extended to 5 μM; the LOD (S/N=3) was determined to be 47 nM (n=7). FigureS5 shows the signal reproducibility for seven successive determinations of 1 mL 2 μM aqueous cyanide, with $A_{160\,s}$ absorbance having a variance of 4.7%.

Bovine Blood—The calibration results for 100 μL of bovine blood containing 0–40 μM CN^- added are shown in Figure S5. The linear range extended to 40 μM (r^2> 0.99); the LOD was 1.0 μM. The signal reproducibility of seven successive determinations of 20 μM cyanide in 100 μL of bovine blood is shown in FigureS6; $A_{160\,s}$ exhibited a variance of 9.7%. Part of this higher variability may come from difficulties in accurate volumetric delivery of bovine blood, a viscous liquid. With an order of magnitude greater sample volume, the variance of A_{160s} decreased to 3.9%. The LOD improves to 0.15 μM for the 1 mL sample volume but the linear range (r^2> 0.99) extended only to 5 μM. Detailed data are shown in Figures S7 and S8. The LOD obtained with a 1 mL sample would be sufficient for measuring cyanide in the blood of healthy individuals not deliberately exposed to cyanide.

Rabbit Blood—The calibration results for 20 μL of rabbit blood containing 0–200 μM CN^- added are shown in Figure S9. The linear range extended to 200 μM and a LOD of 5.0 μM was attained; the RSD was 3.7% at the 100 μM CN^-, n=7; Figure S10). A sample volume of 50 μL, however, provided the most meaningful combination of dynamic range and LOD for the intended application. The linear dynamic range extended to 60 μM with an LOD of 2.2 μM (Figure S11) and the variance at the 40 μM level was 6.6% (n=7; Figure S12).

3.5. Double blind intercomparison

Blood from an experimental animal was provided by the UCI authors, where new cyanide antidotes are being studied. All blood samples taken are 1 mL in volume. The experimental protocol called for taking a baseline blood sample before NaCN infusion is started at 0.33 mg/min (in a matrix of 0.9% NaCl) and continued for 60–85 min. At one point (typically at t=55 min from the beginning of NaCN infusion, the animal is given an antidote (aquohydroxocobinamide in saline) or a placebo (just saline). Blood is obtained at 5,10, 15, 25 and 35 min after starting the cyanide infusion, at the time the antidote/saline is given, and 10 min after the antidote infusion is begun. Each ~2 mL blood sample was split approximately in half. The samples were sent overnight on ice to UCSD and the other set was sent similarly to UTA.

UCSD researchers used a microdiffusion method [25], the limited sample volume permitted only a duplicate measurement. Two separate calibrations on two separate days using aqueous standards were used with each set of the split replicate subsamples. At UTA, the present method was used; the calibration curve was based on rabbit blood spiked with cyanide at various levels. The baseline sample was analyzed in duplicate using 500 μL aliquots, all the others were first analyzed using 50 μL aliquots (n=4), the highest two concentrations were reanalyzed using 20 μL aliquots. The results of this blind intercomparison are shown in Figure 4. The present method allows much better

measurement precision, has a smaller sample requirement and does not require a sophisticated benchtop spectrometer.

3.6. Baseline cyanide levels in healthy humans

Whole blood cyanide levels in 12 healthy nonsmokers, ranged from 0.4 to 1.8 μM (Figure 5). Baseline blood cyanide concentrations, determined by completely unrelated methods reportedly range from 0.13 to 2.9 μM for nonsmokers [52, 53] and 0.27 to 6.8 μM for smokers [53, 54]; our data are well within this norm.

4. Conclusion

Liberation of a volatile analyte from a sample in a closed environment which incorporates a relatively long path optical sensor represents a uniquely useful configuration that automatically provides matrix isolation and is inexpensively implemented. Such a disposable sensor would be attractive for field use, especially emergency and clinical use. The sensor will have an umbilical cord that directly connects to a computer or a microprocessor/reader to provide results. While it is clearly useful for rapid determination of blood cyanide, we believe that even more importantly the general concept is versatile and should be valuable in many other applications. In agricultural/environmental analysis for example, by adding base alone, soil NH_3-N can be released as NH_3 that can be detected by diffusion into an acid-base indicator; by adding Zn dust and NaOH, total nitrogen can be measured. Arsenic content of water can be measured by adding $NaBH_4$, detecting the liberated arsine by monitoring decolorization with a colored oxidant such as MnO_4^-, Ce^{4+}, or I_3^-.

Although the sensor top contains < US $5 in parts, it is easily reused if so desired. Preliminary experiments indicate that instead of pipetting blood into the sample chamber, spotting blood on an absorbent filter/pad and using this filter as sample produces no difference in results. In some situations, using a self-filling capillary on a finger prick and transferring that to a filter prior to analysis may be more expedient.

Acknowledgments

This work was supported in part by the National Institutes of Health Grant No. NINDS U01 NS058030-S3. YT and JHW acknowledges support from the Natural Science Foundation of China (21075013, 20725517, Major International Joint Research Project 20821120292), and the China Scholarship Council (2010608060). We thank Howard Bailiff for his expert assistance.

References

1. Boening DW, Chew CM. Water Air Soil Poll. 1999; 109:67–79.
2. Prabhakaran K, Li L, Borowitz JL, Isom GE. J Pharmacol Exp Ther. 2002; 303:510–519. [PubMed: 12388630]
3. Sousa AB, Soto-Blanco B, Guerra JL, Kimura ET, Gorniak SL. Toxicology. 2002; 174:87–95. [PubMed: 11985886]
4. Xu Z, Chen X, Kim HN, Yoon J. Chem Soc Rev. 2010; 39:127–137. [PubMed: 20023843]
5. Dash RR, Gaur A, Balomajumder C. J Hazard Mater. 2009; 163:1–11. [PubMed: 18657360]
6. Rawel HM, Kroll J. Deut Lebensm-Rundsch. 2003; 99:102–108.
7. Donato DB, Nichols O, Possingham H, Moore M, Ricci PF, Noller BN. Environ Int. 2007; 33:974–984. [PubMed: 17540445]
8. Alarie Y. Crit Rev Toxicol. 2002; 32:259–289. [PubMed: 12184505]
9. De Lorenzo A. JEMS-J Emerg Med Ser. 1999; 24:54–58. 60–61, 64–65.
10. Rotenberg JS. Pediatr Ann. 2003; 32:236–240. [PubMed: 12723118]

11. Ma JA, Dasgupta PK. Anal Chim Acta. 2010; 673:117–125. [PubMed: 20599024]
12. Logue BA, Hinkens DM, Baskin SI, Rockwood GA. Crit Rev Anal Chem. 2010; 40:122–147.
13. Zelder FH, Mannel-Croise C. Chimia. 2009; 63:58–62.
14. Lindsay AE, Greenbaum AR, O'Hare D. Anal Chim Acta. 2004; 511:185–195.
15. Murphy KE, Schantz MM, Butler TA, Benner BA, Wood LJ, Turk GC. Clin Chem. 2006; 52:458–467. [PubMed: 16439606]
16. Lobger LL, Petersen HW, Andersen J. Anal Lett. 2008; 41:2564–2586.
17. Frison G, Zancanaro F, Favretto D, Ferrara SD. Rapid Commun Mass Spectrom. 2006; 20:2932–2938. [PubMed: 16941546]
18. Boadas-Vaello P, Jover E, Llorens J, Bayona JM. J Chromatogr B. 2008; 870:17–21.
19. Felby S. Forensic Sci Med Pathol. 2009; 5:39–43. [PubMed: 19291430]
20. Gambaro V, Arnoldi S, Casagni E, Dell'Acqua L, Pecoraro C, Froldi R. J Forensic Sci. 2007; 52:1401–1404. [PubMed: 18093070]
21. Liu GJ, Liu JT, Hara K, Wang YF, Yu YP, Gao LN, Li L. J Chromatogr B. 2009; 877:3054–3058.
22. Zhang CS, Zheng H, Jin OY, Feng SZ, Taes YEC. Anal Lett. 2005; 38:247–256.
23. Lindsay AE, O'Hare D. Anal Chim Acta. 2006; 558:158–163.
24. Lv J, Zhang ZJ, Li JD, Luo LR. Forensic Sci Int. 2005; 148:15–19. [PubMed: 15607585]
25. Blackledge WC, Blackledge CW, Griesel A, Mahon SB, Brenner M, Pilz RB, Boss GR. Anal Chem. 2010; 82:4216–4221. [PubMed: 20420400]
26. Ma JA, Dasgupta PK, Blackledge W, Boss GR. Anal Chem. 2010; 82:6244–6250. [PubMed: 20560532]
27. Ma J, Ohira S-I, Mishra SK, Puanngam M, Dasgupta PK, Mahon SB, Brenner M, Blackledge W, Boss GR. Anal Chem. 2011; 83:4319–4324. [PubMed: 21553921]
28. Ma J, Dasgupta PK, Zelder FH, Boss GR. Anal Chim Acta. 2012; 736:78–84. [PubMed: 22769008]
29. Ma J, Dasgupta PK, Blackledge W, Boss GR. Environ Sci Technol. 2010; 44:3028–3034. [PubMed: 20302333]
30. Conway EJ, Byrne A. Biochem J. 1933; 27:419–429. [PubMed: 16745115]
31. Conway EJ. Biochem J. 1933; 27:430–434. [PubMed: 16745116]
32. Conway EJ. Biochem J. 1935; 29:2755–2772. [PubMed: 16745964]
33. Conway, EJ. Micro-Diffusion Analysis. Crosby Lockwood; London: 1939.
34. Toda K, Yoshioka KI, Ohira SI, Li JZ, Dasgupta PK. Anal Chem. 2003; 75:4050–4056. [PubMed: 14632117]
35. Skeggs LT. Jr Ann NY Acad Sci. 1960; 87:650–657.
36. Skeggs LT. Jr Am J Clin Path. 1960; 33:181–185.
37. Kenny MA, Cheng MH. Clin Chem. 1972; 18:352–354. [PubMed: 5012257]
38. BaadenHuijsen H, Seuren-Jacobs HEH. Clin Chem. 1979; 25:443–445. [PubMed: 122236]
39. Mattos IL, Luque de Castro MD. Anal Chim Acta. 1994; 298:159–165.
40. Choengchan N, Wilairat P, Dasgupta PK, Motomizu S, Nacapricha D. Anal Chim Acta. 2006; 579:33–37. [PubMed: 17723724]
41. Mornane P, van den Haaka J, Cardwell TJ, Cattrall RW, Dasgupta PK, Kolev SD. Talanta. 2007; 72:741–746. [PubMed: 19071680]
42. Sereenonchai K, Saetear P, Amornthammarong N, Uraisin K, Wilairat P, Motomizu S, Nacapricha D. Anal Chim Acta. 2007; 597:157–162. [PubMed: 17658326]
43. Muncharoen S, Sitanurak J, Tiyapongpattana W, Choengchan N, Choengchan N, Ratanawimarnwong N, Motomizu S, Wilairat P, Nacapricha D. MIcrochim Acta. 2009; 164:203–210.
44. Sereenonchai K, Teerasong S, Chan-Eam S, Saetear P, Choengchan N, Uraisin K, Amornthammarong N, Motomizu S, Nacapricha D. Talanta. 2010; 81:1040–1044. [PubMed: 20298891]

45. Teerasonga S, Chan-Eamb S, Sereenonchai K, Amornthammarong N, Ratanawimarnwonge N, Nacapricha D. Anal Chim Acta. 2010; 668:47–53. [PubMed: 20457301]
46. Klapper MH, Uchida H. J Biol Chem. 1971; 246:6840–6854.
47. Blumenthal DC, Kassner RJ. J Biol Chem. 1980; 255:5859–5863. [PubMed: 6247350]
48. Sano A, Takimoto N, Takitani S. J Chromatogr. 1992; 582:131–135. [PubMed: 1491032]
49. Chinaka S, Takayama N, Michigami Y, Ueda K. J Chromatogr B. 1998; 713:353–359.
50. [Accessed april 3, 2012] International cyanide management code for the gold mining industry. Environmental and health effects of cyanide. http://www.cyanidecode.org/cyanide_environmental.php
51. Baud FJ, Barriot P, Toffis V, Riou B, Vicaut E, Lecarpentier Y, Bourdon R, Astier A, Bismuth C. New Engl J Med. 1991; 325:1761–1766. [PubMed: 1944484]
52. Lundquist P, Rosling H, Sorbo B. Clin Chem. 1985; 31:591–595. [PubMed: 3978792]
53. Symington IS, Anderson RA, Thomson I, Oliver JS, Harland WA, Kerr JW. Lancet. 1978; 2:91–92. [PubMed: 78311]
54. Tsuge K, Kataoka M, Seto Y. J Health Sci. 2000; 46:343–350.

Highlights

- Cyanide in blood is determined in ~4 min by an inexpensive sensor
- As little as 20 μL sample can be used
- The recommended sample volume, 50 μL can be obtained by finger prick
- 50μL blood sample provides for an LOD of 2.2 μM and upper linear limit of 60 μM
- With 1 mL sample, baseline cyanide levels in blood can be measured

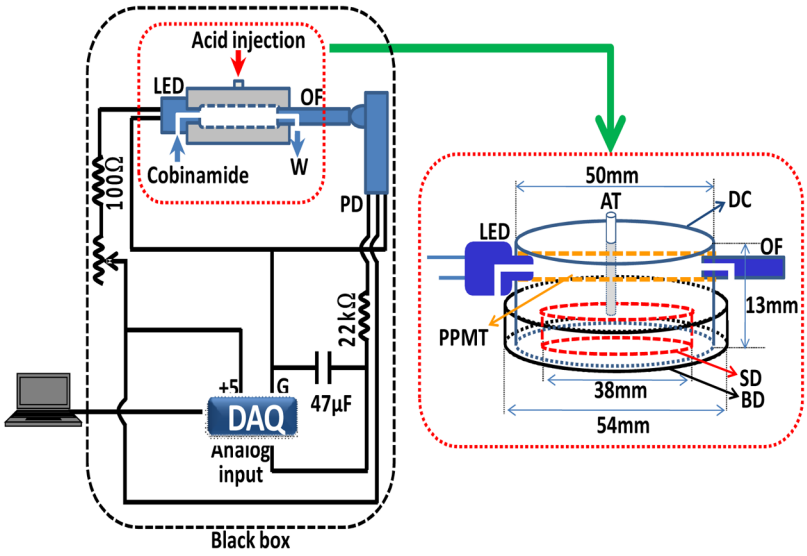

Figure 1.

Diagram of the cyanide measuring device. LED: Light emitting diode (583 nm); OF: optical fiber; PD: photodiode; PPMT: porous polypropylene membrane tube; AT: acid injection tube; DC: detection cell; SD: sample dish; BD: outer bottom dish; DAQ: data acquisition board; W: waste.

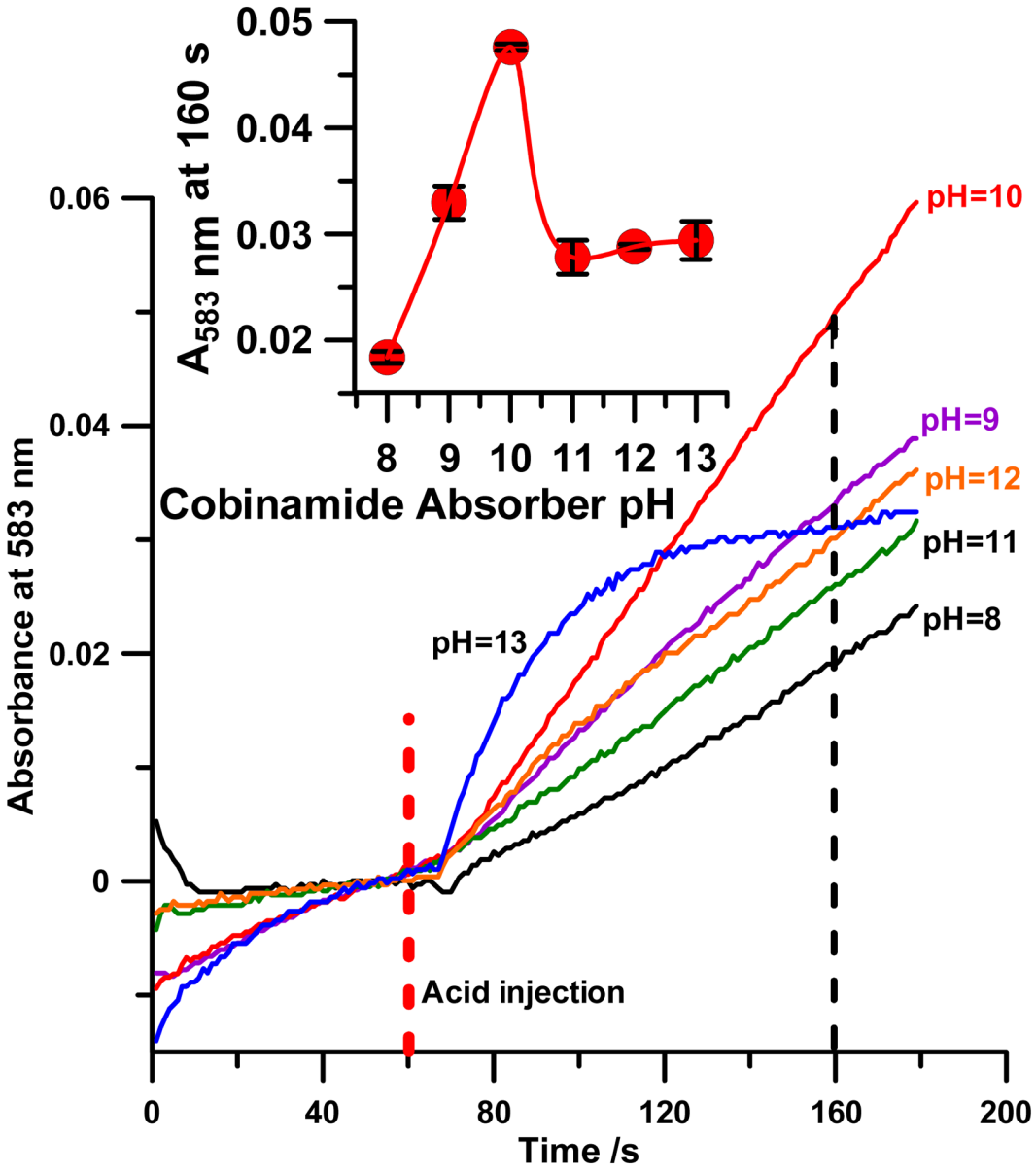

Figure 2.

Influence of the pH of the hydroxocyanocobinamide solution (20 μM) on the temporal development of absorbance at 583 nm, 2 μM aqueous cyanide sample. We normally carried out single point quantitation based on the absorbance at t = 160 s, marked by the vertical arrow. The inset shows the change in this value as a function of absorber pH.

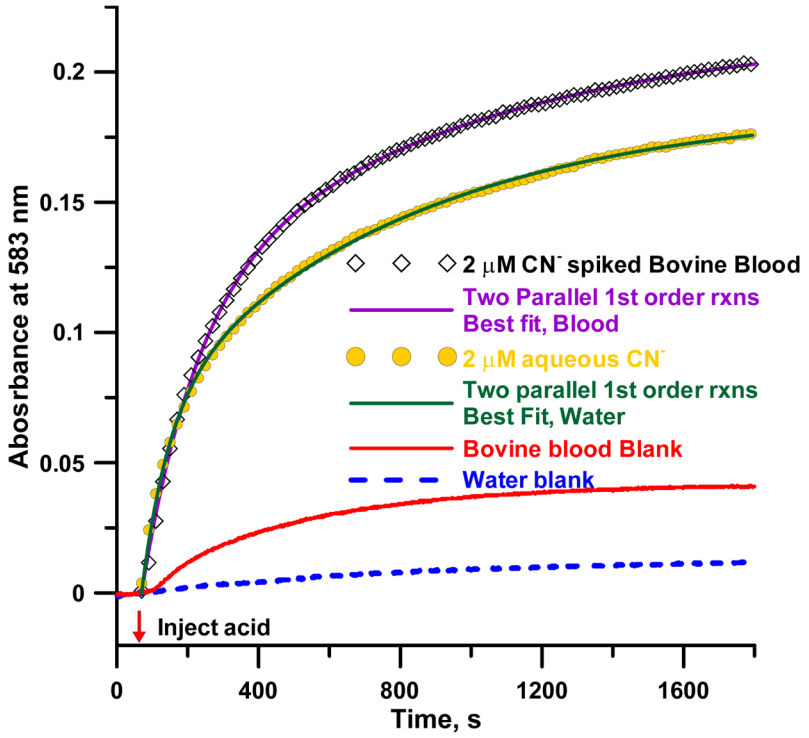

Figure 3.

Time course of spectral changes on adding cyanide to water and blood. (Hydroxocyanocobinamide: 20 μM in 0.01 M borate buffer pH 10; diamonds: 1 mL bovine blood spiked with CN^- to 2 μM; circles: 1 mL 2 μM aqueous cyanide adjusted to pH 12. The solid lines running through the points show the respective best fits to equation 1. The blank water and bovine blood runs clearly indicate presence of cyanide in the blood sample.)

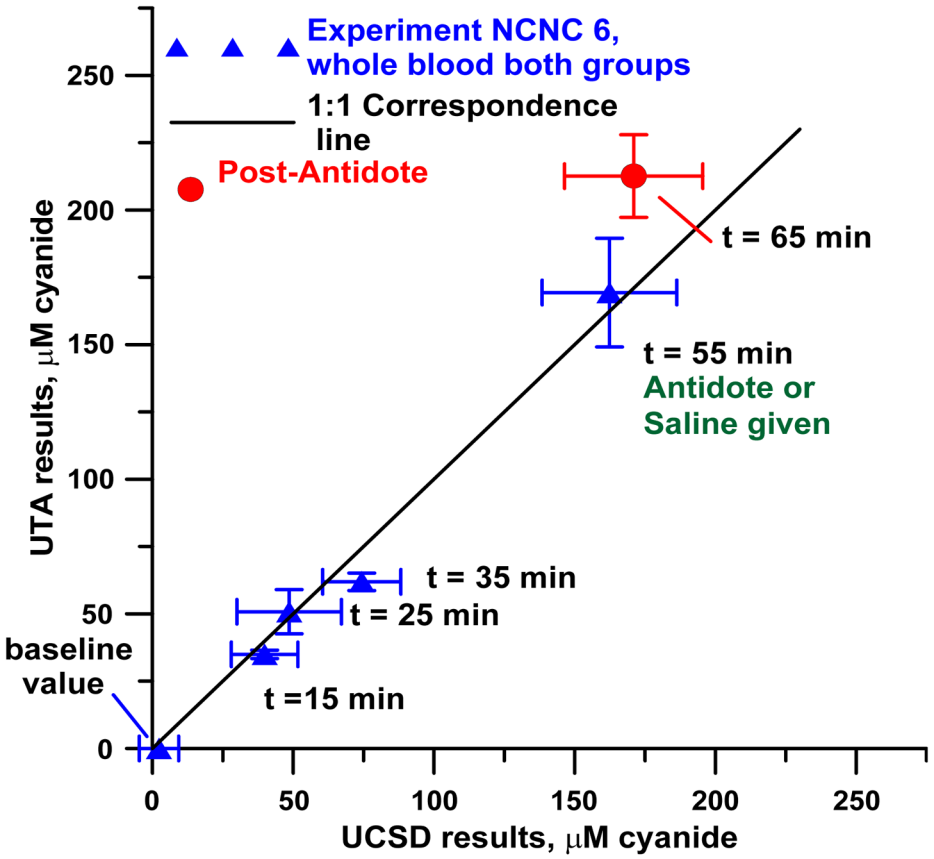

Figure 4.
Comparison of blood cyanide concentrations measured at UCSD and UTA by two different methods. Experimental rabbit at UCI was infused with 0.33 mg/min cyanide and samples taken at different times. See text for details.

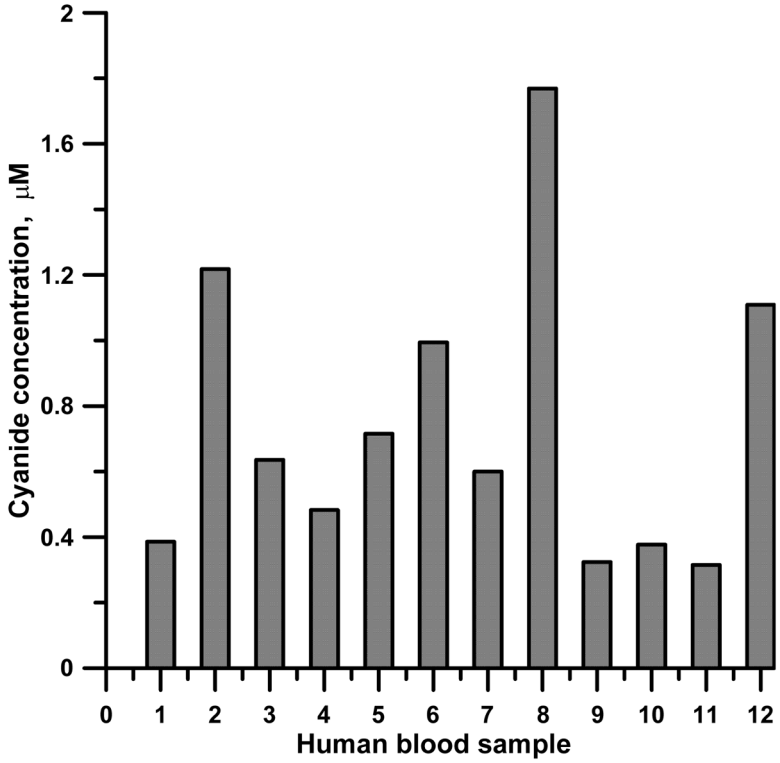

Figure 5.
Cyanide concentration in blood of 12 healthy adult nonsmokers. 1 mL blood injection, other experimental conditions were as shown in Table S1.